which the van der Waals radii of the atoms are used indicates that the Na^+ ion is completely encased by the coiled PEG9.

The experimental data for other systems are given in Fig. 4 as a plot of K_o^{-1} versus the number of monomers. A regular, near-linear increase with monomer number is observed as expected for members of a single structural family (*17*). We have modeled Na^+PEG13 and Na^+PEG17 in addition to Na^+PEG9, and these three data points are shown in Fig. 4 for comparison. Excellent agreement was obtained between the model and experiment. Modeling of the complete series will be reported elsewhere (*13*).

The Sybyl molecular mechanics programs were also used to model the possible stable conformers of the neutral PEG9. A series of 400 stable conformers were randomly generated with resulting relative energies over a range of ~20 kcal mol^{-1}. Several of the more stable species were annealed and subjected to energy minimization. The most stable of these was then subjected to 200,000 fs of molecular dynamics at 300 K, and 2000 structures were extracted at 100-fs intervals. The mobilities these species would have generated if singly charged were in the range $K_o = 3.5 \pm 0.4$ cm^2 V^{-1} s^{-1}. This lower value of K_o indicates that a much more open structure is predicted for neutral PEG9 relative to Na^+PEG9, and the molecular dynamics simulation reveals that a much wider range of conformers is sampled at 300 K. Both results are consistent with rather weak intramolecular interactions in neutral PEG9 relative to Na^+PEG9.

A few words of comparison with our bradykinin results (*12*) are useful. Bradykinin is almost exclusively cationized with protons, rather than with Na^+ in our experiments, regardless of the matrix. Protons prefer to form localized bonds, and, if the charge is shared, they usually involve only two centers. Furthermore, bradykinin has two arginine units, one at the NH_2-terminus and one at the COOH-terminus, which are preferred sites of protonation (*22*). Hence, one might expect a more open structure for protonated bradykinin (a nine-residue peptide chain) than for Na^+-cationized PEG structures. Our modeling suggests that this is the case. The experimental mobility is 2.20 ± 0.05 cm^2 V^{-1} s^{-1}, and our preliminary modeling results, assuming protonation at arginine, yield a mobility of ~2.1 cm^2 V^{-1} s^{-1} for the lowest energy structure. The model result needs to be subjected to molecular dynamics averaging, and searches for other possible protonation sites need to be done. Nonetheless, the agreement is remarkably good and lends strong support both for the Sybyl molecular mechanics force field (*18*) and for our method for determining the van der Waals radii of the involved atoms (*19–21*).

REFERENCES AND NOTES

1. F. M. Richards, *Sci. Am.* **264**, 54 (January 1991).
2. M. Karas and F. Hillenkamp, *Anal. Chem.* **60**, 2299 (1988); R. C. Beavis and B. T. Chait, *Rapid Commun. Mass Spectrom.* **3**, 432 (1989); *ibid.*, p. 436.
3. C. M. Whitehouse, R. N. Dreyer, M. Yamashuta, J. B. Fenn, *Anal. Chem.* **57**, 675 (1985); J. B. Fenn, M. Mann, C. K. Meng, S. F. Wong, C. M. Whitehouse, *Science* **264**, 64 (1989).
4. See the special issue on mass spectrometry, *Acc. Chem. Res.* **27**, issue 11 (November 1994).
5. See, for example, B. T. Chait, R. Wang, R. C. Beavis, S. B. H. Kent, *Science* **262**, 89 (1993); K. Biemann, *Fresenius Z. Anal. Chem.* **343**, N1:25 (1992); *Annu. Rev. Biochem.* **61**, 977 (1992).
6. For leading references on alkali metals and peptides, see: R. B. Cody, J. I. Amster, F. W. McLafferty, *Proc. Natl. Acad. Sci. U.S.A.* **82**, 6367 (1985); L. M. Mallis and D. H. Russell, *Anal. Chem.* **58**, 1076 (1986); X. Tang, W. Eus, K. G. Standing, J. B. Westmore, *ibid.* **60**, 1791 (1988); R. P. Grese, R. L. Cerny, M. L. Gross, *J. Am. Chem. Soc.* **111**, 2835 (1989); J. A. Leary, T. D. Williams, G. Bott, *Rapid Commun. Mass Spectrom.* **3**, 192 (1989); L. M. Teesch and J. Adams, *J. Am. Chem. Soc.* **113**, 812 (1991).
7. For leading references on alkaline earth and transition metal ions, see: L. M. Teesch and J. Adams, *J. Am. Chem. Soc.* **112**, 4110 (1990); P. Hu and M. L. Gross, *ibid.* **114**, 9153 (1992); H. Zhoo, A. Reiter, L. M. Teesch, J. Adams, *ibid.* **115**, 2854 (1993); P. Hu and M. L. Gross, *ibid.*, p. 8821.
8. S. K. Chowdhung, V. Katta, B. T. Chait, *ibid.* **112**, 9012 (1990); J. A. Loo, R. R. Ogorzalek-Loo, H. R. Udseth, C. G. Edmunds, R. D. Smith, *Rapid Commun. Mass Spectrom.* **5**, 101 (1991); R. Gueuremont, K. W. M. Sui, J. C. Y. LeBlanc, S. S. Berman, *J. Am. Soc. Mass Spectrom.* **3**, 216 (1992).
9. V. Katta and B. T. Chait, *Rapid Commun. Mass Spectrom.* **5**, 214 (1991); B. E. Winger, K. J. Light-Wahl, A. L. Rockwood, R. D. Smith, *J. Am. Chem. Soc.* **114**, 5897 (1992); D. Suekau *et al.*, *Proc. Natl. Acad. Sci. U.S.A.* **90**, 790 (1993).
10. T. Covey and D. J. Douglas, *J. Am. Soc. Mass Spectrom.* **4**, 616 (1993); K. A. Cox, R. K. Julian, R. G. Cooks, R. E. Kaiser, *ibid.* **5**, 127 (1994).
11. M. T. Bowers, P. R. Kemper, G. von Helden, P. A. M. van Koppen, *Science* **260**, 1446 (1993).
12. T. Wyttenbach, G. von Helden, M. T. Bowers, unpublished results.
13. G. von Helden, T. Wyttenbach, M. T. Bowers, *Int. J. Mass Spectrom. Ion Processes* (Al Nier special issue), in press.
14. P. R. Kemper and M. T. Bowers, *J. Am. Soc. Mass Spectrom.* **1**, 197 (1990).
15. ———, *J. Phys. Chem.* **95**, 5134 (1991).
16. E. A. Mason and E. W. McDaniel, *Transport Properties of Ions in Gases* (Wiley, New York, 1988).
17. G. von Helden, M.-T. Hsu, N. Gotts, M. T. Bowers, *J. Phys. Chem.* **97**, 8182 (1993).
18. M. Clark, R. D. Cramer III, N. van Opdenbosch, *J. Comput. Chem.* **10**, 982 (1989).
19. The van der Waals radii used were 1.09 Å for He, 1.51 Å for O, 1.10 Å for H, and 1.61 Å for C. The He and C van der Waals radii were the same as those used for very extensive C studies (*17*). The H and O radii were determined by He scattering calculations on CH_4 and $(C_2H_5)_2O$, respectively. More details are given in (*20*) and (*21*).
20. G. von Helden, E. Porter, N. G. Gotts, M. T. Bowers, *J. Phys. Chem.* (Mostafa El Sayed special issue), in press.
21. G. von Helden, thesis, University of California at Santa Barbara (1994).
22. G. S. Gorman, J. P. Speir, C. A. Turner, I. J. Amster, *J. Am. Chem. Soc.* **114**, 3986 (1992).

23. This work was supported under NSF grants CHE91-10752 and CHE94-21176 and by the Air Force Office of Scientific Research under grant FA 9620-93-1-0134.

13 October 1994; accepted 10 January 1995

Control of IκB-α Proteolysis by Site-Specific, Signal-Induced Phosphorylation

Keith Brown, Susan Gerstberger, Louise Carlson, Guido Franzoso, Ulrich Siebenlist*

IκB-α inhibits transcription factor NF-κB by retaining it in the cytoplasm. Various stimuli, typically those associated with stress or pathogens, rapidly inactivate IκB-α. This liberates NF-κB to translocate to the nucleus and initiate transcription of genes important for the defense of the organism. Activation of NF-κB correlates with phosphorylation of IκB-α and requires the proteolysis of this inhibitor. When either serine-32 or serine-36 of IκB-α was mutated, the protein did not undergo signal-induced phosphorylation or degradation, and NF-κB could not be activated. These results suggest that phosphorylation at one or both of these residues is critical for activation of NF-κB.

Proteolytic degradation of IκB-α is essential for activation of NF-κB (*1–4*). When degradation is blocked by certain protease inhibitors that target proteasomes, activation of NF-κB is prevented. Physiologic stimulation also induces phosphorylation of IκB-α (*1–7*), but the significance of this phosphorylation for activation of NF-κB in cells has remained unclear. Induced phosphorylation does not in itself dissociate complexes of IκB-α and NF-κB in vivo (*1, 2, 4, 7*). The question arises as to how proteolysis of IκB-α is triggered.

To identify regions in IκB-α essential for signaling and degradation, we systematically mutated the human IκB-α gene and stably transfected the altered genes into mouse EL-4 T lymphocytes (*8–10*). Human IκB-α was distinguished from endogenous murine IκB-α by its slower mobility on SDS gels. The exogenous human wild-type IκB-α and endogenous murine IκB-α were degraded with similar kinetics upon cellular stimula-

Laboratory of Immunoregulation, National Institute of Allergy and Infectious Diseases, National Institutes of Health, Building 10, Room 11B16, Bethesda, MD 20892–1876, USA.

*To whom correspondence should be addressed.

tion with tumor necrosis factor–α (TNF-α) (Fig. 1A) or phorbol 12-myristate 13-acetate (PMA) + ionomycin (Fig. 1B). Furthermore, the human IκB-α was phosphorylated in a signal-dependent manner, as indicated by the characteristic shift in electrophoretic mobility that accompanies signal-induced phosphorylation of endogenous IκB-α from human cells (*2*) (Fig. 2, A and D). To block proteolysis in the latter experiments, we added calpain inhibitor I to the cells (*11*). Although murine IκB-α was also phosphorylated upon stimulation (see below), only a small change in mobility was observed. The proteolysis and phosphorylation tests established that permanently transfected human wild-type IκB-α is fully signal-responsive in these cells.

We then tested various deletions and point mutants of human IκB-α in EL-4 cells (*10*). A deletion mutant missing the NH_2-terminal 54 amino acids (ΔN) was neither proteolyzed nor phosphorylated in response to signals (Figs. 1B and 2B), but still fully inhibited NF-κB (Fig. 3A). We therefore investigated potential phosphoacceptor sites within the deleted portion. IκB-α containing a Ser^{32}→Gly mutation (mt^{32}) was not degraded upon stimulation by TNF-α or PMA + ionomycin (Fig. 1D) (*12*) nor did it undergo the characteristic mobility shift upon cellular stimulation, suggesting a defect in signal-induced phosphorylation (Fig. 2D). IκB-α containing a Ser^{36}→Ala mutation (mt^{36}) behaved similarly (Figs. 1E and 2E). Both mutants still inhibited NF-κB, as determined by transient transfection of human NTera-2 embryonal carcinoma cells with a κB-dependent reporter plasmid (*9*) (Fig. 3A) and by in vitro DNA binding assays (Fig. 3B) (*12*). The mt^{32} IκB-α was also precipitated from EL-4 cell extracts with antibodies against the p65 subunit of NF-κB, regardless of whether cells were stimulated (Fig. 3C). We conclude that a mutation at either Ser^{32} or Ser^{36} (or deletion of the NH_2-terminus) has no effect on the inhibitory function of IκB-α but completely abolishes the signal-induced, phosphorylation-dependent shift in mobility and the degradation of IκB-α.

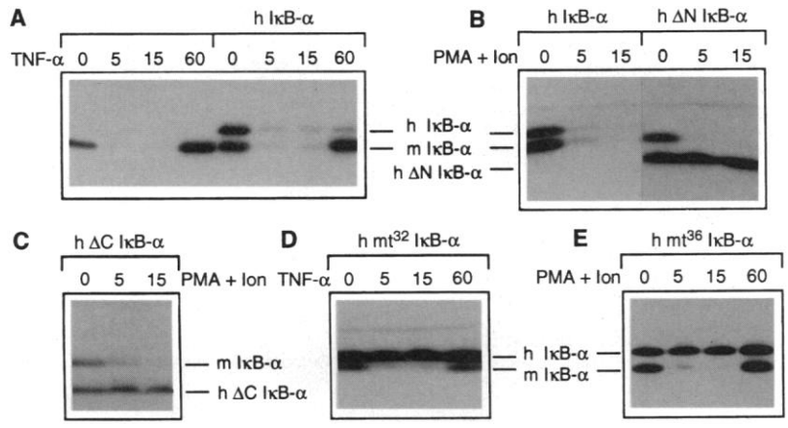

Fig. 1. (**A** to **E**) Signal-induced proteolysis of endogenous murine (m) and exogenous human (h) IκB-α in murine EL-4 T cells. Immunoblots had equal amounts of whole-cell extracts in each lane. Untransfected cells (A, left) or cells stably transfected (*8*) with the indicated IκB-α constructs (*10*) were stimulated with murine TNF-α (2000 U/ml; Genzyme, Cambridge, Massachusetts); or PMA (40 ng/ml; Sigma, St Louis, Missouri) and ionomycin (Ion, 2 μM, Calbiochem, San Diego, California). The numbers above the lanes indicate the period of time (in minutes) between cell stimulation and harvest. Blots A, B, D, and E were probed with rabbit polyclonal antibody directed against the COOH-terminus (amino acids 230 to 315) of h IκB-α. Blot C was probed with rabbit polyclonal antibody against full-length h IκB-α. The mobilities of h IκB-α, mt^{32}, and mt^{36} were similar. In (A), (D), and (E), the time course extends to 60 min after stimulation, at which time m IκB-α has already been resynthesized. This observation is explained by the rapid activation of endogenous m (but not exogenous h) IκB-α transcription by activated NF-κB released through degradation of IκB-α protein (*5*).

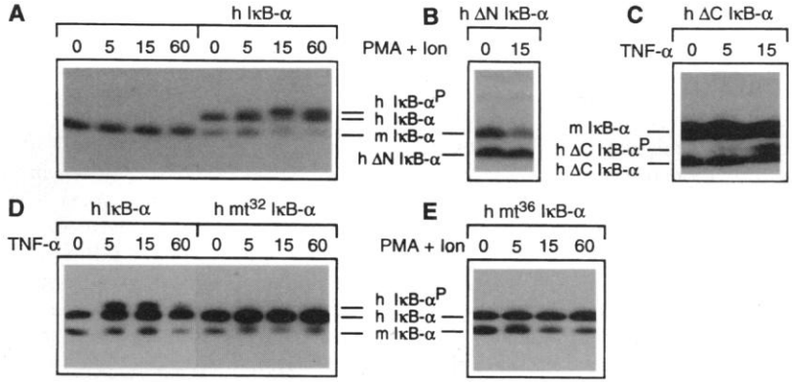

Fig. 2. (**A** to **E**) Signal-induced phosphorylation of h IκB-α in murine EL-4 T cells. Immunoblots were prepared as in Fig. 1. Cells were preincubated for 30 min with Calpain Inhibitor (100 μM, Boehringer, Indianapolis, Indiana) (*2*) prior to stimulation with mTNF-α or PMA + Ion, and later extracted in the presence of phosphatase inhibitors (*2, 5*). The signal-induced phosphorylated species of h IκB-α (h $IκB-α^P$) migrates slightly slower than h IκB-α.

Mutations of all other potential phosphoacceptor Ser, Thr, and Tyr residues in the NH_2-terminal 89 residues of IκB-α (the region NH_2-terminal to the ankyrins and the beginning of the ankyrin domain) did not block signal-induced phosphorylation or degradation of the protein, nor did mutations of several other residues located elsewhere in the protein (*13*). These results support the hypothesis that Ser^{32} and Ser^{36} mutants directly blocked phosphorylation at one or both of these sites. (*14*). Proteolysis of the inhibitor also appears to require sequences at the COOH-terminus of IκB-α. A mutant missing the 41 COOH-terminal residues (ΔC) was not proteolyzed in response to signals but was phosphorylated (Figs. 1C and 2C), indicating that induced phosphorylation is necessary but not sufficient for proteolysis. The ΔC deletion eliminated sequences rich in Pro, Glu/Asp, Ser, and Thr residues (PEST sequences), which are often found in proteins that turn over rapidly (*15, 16*) and which may be necessary for induced proteolysis of IκB-α. The ΔC mutant still inhibited NF-κB activity in transfection experiments and retained its ability to bind p65, but it did not inhibit DNA binding of NF-κB in vitro (Fig. 3B) (*12, 17*). Thus, cytoplasmic retention of NF-κB and inhibition of DNA binding appear to be separable functions of IκB-α, with the latter requiring additional COOH-terminal sequences.

The mutations blocking signal-induced phosphorylation and proteolysis also prevented activation of NF-κB. We demonstrated this in NTera-2 cells, which do not express endogenous NF-κB or IκB-α (Fig. 3A) (*9*). Transactivation of a κB-driven reporter, which is dependent on cotransfection of the p65 subunit of NF-κB, was inhibited by cotransfection of wild-type IκB-α as well as by the mutants ΔN, mt^{32}, and mt^{36}. Upon stimulation with PMA + ionomycin, inhibition of NF-κB transactivation was relieved in the cells transfected with wild-type IκB-α, but not in those transfected with the signal-defective mutants.

Two-dimensional gel analyses were performed to separate phosphoisoforms of metabolically labeled human IκB-α (*18*). When immunoprecipitated from unstimulated EL-4 cells, ^{35}S-labeled wild-type human IκB-α resolved into several isoforms, revealed as a string of spots (Fig. 4A). Similar isoforms were also observed with murine IκB-α from unstimulated cells (*18*) and with mt^{32} (Fig. 4B). The spots represent distinct IκB-α phosphoisoforms that differ in the extent of phosphorylation. With prior phosphatase treatment, the spots collapsed into a single spot (*18*). Metabolic labeling with [^{32}P]orthophosphate confirmed that IκB-α was phosphorylated in unstimulated cells, with the more phosphorylated isoforms represented by the more intense spots (Fig. 4C). The significance of this constitutive phosphorylation is unknown.

Upon cellular stimulation, the constitutive phosphoisoforms of IκB-α were further phosphorylated, resulting in the appearance of additional spots with slower mobility in the second (size) dimension. The shift of these new spots toward a lower pH in the first dimension was consistent with a more negative charge (Fig. 4A). This was confirmed with ^{32}P-labeled IκB-α (Fig. 4C). The apparent magnitude of the shift in the first dimension suggests that more than one phosphate was added in response to signals (Fig. 4, A and C). In contrast to wild-type IκB-α, the mt^{32} (Fig. 4B) ΔN, and mt^{36} mutants (*18*) exhibited no apparent phosphorylation changes in response to cellular stimulation.

These data indicate that signal-induced phosphorylation of IκB-α is necessary for proteolysis of the inhibitor and for activation of NF-κB. Conservative mutations at either Ser^{32} or Ser^{36} blocked phosphorylation and degradation of IκB-α. These residues in IκB-α have been highly conserved through evolution (*19*). The most direct interpretation of our data is that NF-κB activating signals lead to phosphorylation, possibly at both Ser^{32} and Ser^{36} (*20*), which in turn represents a recognition signal that is necessary but not sufficient for proteolysis. Proteolysis of IκB-α requires additional sequences, including a COOH-terminal PEST region. Site-specific, signal-induced phosphorylation of proteins may be a general mechanism for rapidly altering protein stability in response to extracellular stimuli or during the cell cycle.

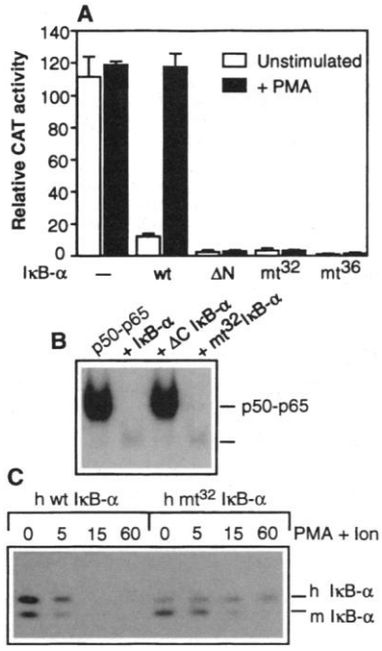

Fig. 3. Functional interaction of h IκB-α mutants with NF-κB. (**A**) Inhibition of NF-κB activation by h IκB-α Ser^{32} or Ser^{36} mutants. NTera-2 cells were transiently transfected with NF-κB p65 (0.2 μg, PMT2T-p65) and with a chloramphenicol acetyltransferase (CAT) reporter plasmid (5 μg) containing the κB site derived from human immunodeficiency virus (HIV) (*9*). Wild-type (wt) h IκB-α and h IκB-α mutants ΔN, mt^{32}, and mt^{36} (0.1 μg each on vector PMT2T) were cotransfected. Cells were stimulated for 6 hours with PMA (10 ng/ml) and 36 hours after transfection, they were harvested, extracted, and assayed for CAT activity (*9*). The values shown are the means of three independent experiments. Relative CAT activity refers to fold transactivation relative to cells transfected with reporter plasmid alone. (**B**) Inhibition of binding of NF-κB to κB-DNA by h IκB-α mutants. Extracts of NTera-2 cells cotransfected with NF-κB p50 and p65 (3 μg each vector) and with IκB-α constructs (4 μg each vector) were tested in electrophoretic mobility shift assays for binding to a ^{32}P-labeled palindromic κB DNA probe (*9*). The position of p50 homodimers (only faintly visible) is indicated by the mark below the p50-p65 band. (**C**) Physical association of h wt IκB-α and h mt^{32} IκB-α with endogenous murine NF-κB p65. Murine EL-4 T cells stably transfected with these IκB-α constructs were stimulated with PMA (40 ng/ml) + Ion (2 μM). After the indicated period of time (0 to 60 min), they were extracted and immunoprecipitated with protein A–Sepharose beads (Pharmacia, Piscataway, New Jersey) and rabbit polyclonal antibody directed against amino acids 103 to 194 of human p65. Washed precipitates were subjected to electrophoresis, immunoblotted, and probed with rabbit polyclonal antibodies directed against residues 230 to 315 of h IκB-α and ^{125}I-labeled protein A (Dupont, Boston, Massachusetts). The presence of cycloheximide (20 μg/ml) during stimulation blocked the resynthesis of m IκB-α that was usually observed within 60 min (see Fig. 1).

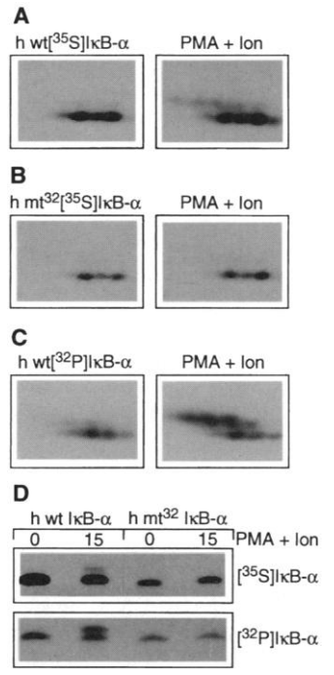

Fig. 4. (**A** to **C**) Two-dimensional gel electrophoresis of h wt IκB-α and h mt^{32} IκB-α. Murine EL-4 T cells stably transfected with these IκB-α constructs were labeled with [^{35}S]methionine plus [^{35}S]cysteine (1 mCi/ml each) or with [^{32}P]orthophosphate (2 mCi/ml) (Dupont, Boston, Massachusetts) for 60 min in the presence of Calpain Inhibitor I (200 μM). Half of each labeled cell suspension was then stimulated for 15 min with PMA (50 ng/ml) plus Ion (4 μM) and extracts were prepared in the presence of phosphatase inhibitors (*2, 5*). Extracts were then immunoprecipitated with a rabbit polyclonal antibody directed against amino acids 6 to 20 of h IκB-α (Santa Cruz Biotechnology, Inc., Santa Cruz, California). This antibody did not cross-react with endogenous m IκB-α (*12*). Immunoprecipitates were then subjected to two-dimensional gel electrophoresis (*18*). The horizontal axis represents the isoelectric focusing dimension. The more acidic species are on the left and the more basic species are on the right. The vertical axis represents the size-separation dimension. (**D**) One-dimensional gel electrophoresis of the ^{35}S- and ^{32}P-labeled h IκB-α immunoprecipitates shown in (A) to (C).

REFERENCES AND NOTES

1. U. Siebenlist, G. Franzoso, K. Brown, *Annu. Rev. Cell Biol.* **10**, 405 (1994).
2. Y.-C. Lin, K. Brown, U. Siebenlist, *Proc. Natl. Acad. Sci. U.S.A.* **92**, 552 (1995).
3. V. J. Palombella, O. J. Rando, A. L. Goldberg, T. Maniatis, *Cell* **78**, 773 (1994).
4. E. B.-M. Traenckner, S. Wilk, P. Baeuerle, *EMBO J.* **13**, 5433 (1994).
5. K. Brown, S. Park, T. Kanno, G. Franzoso, U. Siebenlist, *Proc. Natl. Acad. Sci. U.S.A.* **90**, 2532 (1993).
6. A. A. Beg, T. S. Finco, P. V. Nantermet, A. S. Baldwin, *Mol. Cell. Biol.* **13**, 3301 (1993); S.-C. Sun, P. A. Ganchi, C. Béraud, D. W. Ballard, W. C. Greene, *Proc. Natl. Acad. Sci. U.S.A.* **91**, 1346 (1994).
7. S.-C. Sun, J. Elwood, C. Béraud, W. C. Greene, *Mol. Cell. Biol.* **14**, 7377 (1994); T. S. Finco, A. A. Beg, A. S. Baldwin, *Proc. Natl. Acad. Sci. U.S.A.* **91**, 11884 (1994).
8. The IκB-α genes were transfected into EL-4 cells on vector PMT2T (*9*) by electroporation [20 μg DNA and 10^7 cells, Bio-Rad (Hercules, CA), 250 V, 960 μF], together with a plasmid conferring neomycin (neo) resistance (2 μg). Stable neo^r transfectants were selected by incubation of the electroporated cells for 3

to 4 weeks in medium supplemented with geneticin G418 [(Gibco-BRL, Gaithersburg, MD), at 400 μg/ml for 1 week; 200 μg/ml, 2 to 3 weeks] and then screened for human IκB-α by immunoblotting. The results with each transfected IκB-α species were confirmed with independently transfected cell clones.
9. V. Bours *et al.*, *Mol. Cell. Biol.* **12**, 685 (1992); G. Franzoso *et al.*, *Nature* **359**, 339 (1992); V. Bours *et al.*, *Cell* **72**, 729 (1993).
10. We constructed the ΔN and ΔC IκB-α mutants by cloning into PMT2T (*9*) the 1296–base pair (bp) Xho I–Eco RI fragment and the 921-bp Eco RI–Xmn I fragment, respectively, of the human gene (*15*). Point mutants of IκB-α were obtained in a Bluescript plasmid (Stratagene, La Jolla, CA) containing nucleotides 1 to 1550 of IκB-α complementary DNA (*15*) by site-directed mutagenesis [P. Bressler *et al.*, *J. Virol.* **67**, 288 (1993)]; the mutants were then cloned into PMT2T as 1550-bp Eco RI fragments encoding full-length IκB-α.
11. To permit detection of the newly phosphorylated IκB-α in this experiment, we included phosphatase inhibitors during cell extraction (*2, 5*). To enhance detection, we trapped the phosphorylated intermediate by blocking proteolysis with calpain inhibitor I (*2*).
12. K. Brown, S. Gerstberger, L. Carlson, G. Franzoso, U. Siebenlist, unpublished data.
13. These include all four other potential phosphoacceptor sites within the NH_2-terminal 89 amino acids (residues Tyr^{42}, Ser^{63}, Thr^{71}, and Ser^{76}) and other sites throughout the ankyrin and COOH-terminal domain. Of note, mutation of the protein kinase C consensus site (residues Ser^{262} and Thr^{263}) (*15*) did not prevent activation of NF-κB (*12*).
14. Proteolytic mapping experiments confirmed that induced phosphorylation of IκB-α occurred at a site or sites that are NH_2-terminal to the ankyrin domain (*12*). Thus together with the observation that mutations of all other potential phosphorylation sites within the NH_2-terminal domain of IκB-α did not block signaling indicates that the possibility that the Ser^{32} and Ser^{36} mutations act directly at one or both of these sites to block phosphorylation.
15. S. Haskill *et al.*, *Cell* **65**, 1281 (1991).
16. S. Rogers, R. Wells, M. Rechsteiner, *Science* **234**, 364 (1986).
17. A similar ΔC mutant has previously been shown to inhibit DNA binding of NF-κB in vitro [E. N. Hatada, M. Naumann, C. Scheidereit, *EMBO J.* **12**, 2781 (1993)].
18. Two-dimensional gel electrophoresis was performed as described [P. H. O'Farrell, *J. Biol. Chem.* **250**, 4007 (1975)] by Kendrick Labs, Inc. (Madison, WI). The gels of ^{35}S-labeled murine IκB-α revealed constitutive phosphoisoforms analogous to those of human IκB-α. These experiments also showed that the murine IκB-α was phosphorylated in response to signals (shown by a shift in charge toward negative pH in the first dimension) and that the induced phosphorylation of this species resulted in only a minor shift in apparent size (*12*). Analyses of the ΔN and mt^{36} mutants yielded results similar to those obtained with mt^{32} (*12*). Phosphatase treatment resulted in a single spot (*12*). Endogenous IκB-α from human cells was indistinguishable from exogenously expressed human IκB-α on these gels.
19. R. de Martin *et al.*, *EMBO J.* **12**, 2773 (1994).
20. It remains to be determined if one or both serines are phosphorylated. Mutation of one of these closely spaced serines may block phosphorylation of the other; even if both serines are phosphorylated, their phosphorylation may be linked.
21. We thank K. Kelly and A. S. Fauci for review of the manuscript, A. S. Fauci for continued support, and Y. Ward for expert help and advice.

30 December 1994; accepted 9 February 1995

Requirement of RNA Polymerase III Transcription Factors for in Vitro Position-Specific Integration of a Retroviruslike Element

Jacqueline Kirchner, Charles M. Connolly, Suzanne B. Sandmeyer*

The yeast retroviruslike element Ty3 inserts at the transcription initiation sites of genes transcribed by RNA polymerase III (Pol III). An in vitro integration assay was developed with the use of Ty3 viruslike particles and a modified *SUP2* tyrosine transfer RNA ($tRNA^{Tyr}$) gene target. Integration was position-specific and required Ty3 integrase, Pol III transcription extract, and a transcriptionally competent tRNA gene. Use of individual transcription factor (TF) IIIB–, TFIIIC-, and Pol III–containing fractions showed that TFIIIB and TFIIIC, together, were sufficient for position-specific Ty3 integration, but not for transcription. This report demonstrates that in vitro integration of a retroelement can be targeted by cellular proteins.

Integration of replicated DNA into the host genome is essential for retroviruses and retrotransposons. Integration is nonrandom, but the mechanisms that determine the positions of integration remain poorly defined [reviewed in (*1, 2*)]. DNA sequence, chromatin structure, and the presence of host cell proteins can influence target site selection. On the basis of some in vivo studies, retroviral integration appears to occur preferentially into regions that contain deoxyribonuclease I (DNAase I) hypersensitive sites and regions that are transcriptionally active. A study of avian leukosis virus integration in vivo suggested that most or all of the cellular genome was accessible to integration machinery, but that regional and site preferences existed (*3*). In a series of selected integrations, the yeast retroviruslike element Ty1 integrated with a preference for the 5′ portions of the three RNA Pol II–transcribed genes examined (*4*). In addition, unselected transposition of Ty1 into chromosome III revealed an insertion bias for regions near tRNA genes and outside of open reading frames; this pattern was not observed in vitro with a naked DNA substrate (*5*). These findings have implicated host DNA-associated proteins in integration site selection.

DNA structure influences retroviral integration site selection. This was suggested by a study that identified in vivo integration sites in DNA fragments containing bends (*6*). In addition, in vitro data indicate that integration occurs preferentially into particular DNA structures. Integration mediated by human immunodeficiency virus (HIV) pre-integration complexes or purified integrase (IN) occurred nonrandomly into unmodified, naked DNA and preferentially into runs of CpG modified by 5-methylation of cytosine (*7*). With nucleoprotein complexes of murine leukemia virus (MLV), integration into naked DNA also occurred nonrandomly and more frequently into the exposed major groove of DNA assembled into nucleosomes (*8*). Moreover, DNA positions predicted to be distorted within the nucleosome were used preferentially for integration mediated by HIV IN (*9*). Preferred integration into static or induced bends that were not associated with nucleosomes occurred with both MLV and HIV IN (*10*).

Ty3, a retroviruslike element in *Saccharomyces cerevisiae*, integrates solely upstream of genes transcribed by Pol III. The gene-proximal joint in the host DNA occurs within one to three nucleotides of the transcription initiation site (*11, 12*). On the basis of in vivo experiments, it has been suggested that integration is mediated by a protein-protein interaction between the Ty3 integration complex and the Pol III transcription complex. To identify cellular factors required for Ty3 integration, we developed an in vitro assay. Ty3 viruslike particles (VLPs), analogous to retroviral core particles, were isolated as a complex fraction containing Ty3 RNA, replicated DNA, and the mature Ty3 proteins, including IN (*13*). The target plasmid, pDLC374 (Fig. 1A), was used previously as a target for Ty3 transposition in vivo monitored by genetic selection (*12*) or by a polymerase chain reaction (PCR) assay (*14*). This plasmid contained the yeast *HIS3* gene, a 2-μm plasmid origin of replication, and a modified version of the *SUP2* $tRNA^{Tyr}$ gene cloned into pIBI20. To reconstitute the natural genomic targets of Ty3, we prepared a Pol III transcription extract from yeast cells (*15*). The BioRex70 500 mM NaCl fraction (BR500) from this preparation was used together with Ty3 VLPs and the tRNA gene target plasmid for in vitro integration reactions (*16*). DNA was isolated from each reaction and amplified by PCR with primers

Department of Microbiology and Molecular Genetics, University of California, Irvine, CA 92717, USA.

*To whom correspondence should be addressed.